Published in final edited form as:

ChemMedChem. 2019 February 05; 14(3): 322–333. doi:10.1002/cmdc.201800658.

Microtubule-Targeting 7-Deazahypoxanthines Derived from Marine Alkaloid Rigidins: Exploration of the *N*3 and *N*9 Positions and Interaction with Multi-Drug Resistance Proteins

Ramesh Dasari[a,1], **Andrzej Błauż**[b,1], **Derek C. Medellin**[a], **Roaa M. Kassim**[c], **Carlos Viera**[d], **Maximo Santarosa**[d], **Danielle Turner**[d], **Alet E. van der Westhuyzen**[e], **Willem A. L. van Otterlo**[e], **Taryn Olivas**[a], **Tugba Yildiz**[f], **Tania Betancourt**[a,f], **Charles B. Shuster**[c], **Snezna Rogelj**[d], **Błażej Rychlik**[b,*], **Todd Hudnall**[a,*], **Liliya V. Frolova**[d,*], and **Alexander Kornienko**[a,*]

[a]Department of Chemistry and Biochemistry, Texas State University, San Marcos, Texas 78666, (USA) [b]Cytometry Lab, Department of Molecular Biophysics, Faculty of Biology and Environmental Protection, University of Łódź, ul. Pomorska 141/143, 90-236 Łódź, (Poland) [c]Department of Biology, New Mexico State University, Las Cruces, NM 88003, USA [d]Departments of Chemistry and Biology, New Mexico Tech, Socorro, NM 87801, USA [e]Department of Chemistry and Polymer Science, University of Stellenbosch, ZA-7602 Stellenbosch, South Africa [f]Materials Science and Engineering Program, Texas State University, San Marcos, Texas 78666

Abstract

Our laboratories have been investigating synthetic analogues of marine alkaloid rigidins possessing promising anticancer activities. These analogues, based on the 7-deazahypoxanthine skeleton are available in one- or two-step synthetic sequences and exert cytotoxicity by disrupting microtubule dynamics in cancer cells. In the present work we extended the available structure-activity relationship data to *N*3- and *N*9-substituted derivatives. Although the *N*3-substitution results in a loss of activity, the *N*9-substituted compounds retain the nanomolar antiproliferative activities and antitubulin mode of action of the original unsubstituted compounds. Furthermore, work reported herein also demonstrated that MDR proteins do not confer resistance to both *N*9-unsubstituted and substituted compounds. It was found that sublines overexpressing ABCG2, ABCC1 and ABCB1 proteins were equally responsive to the rigidin analogues as their parental cell lines. Thus, the study reported herein provides further impetus to investigate the rigidin-inspired 7-deazahypoxanthines as promising anticancer agents.

Graphical Abstract

*Co-corresponding authors.
1Co-first authors

Keywords

alkaloids; antitumor agents; 7-deazapurines; drug discovery; pyrrolo[2,3-*d*]pyrimidines

Introduction

Alkaloids isolated from various marine organisms have been found to possess various biological activities and in many cases promising anticancer properties.[1–4] For example, trabectedin (Yondelis®) isolated from the sea squirt *Ecteinascidia turbinata* is currently used to treat patients with advanced soft tissue sarcoma and recurrent platinum-sensitive ovarian cancer in combination therapy.[5–7] Recently, it was also approved by the FDA for the treatment of liposarcoma and leiomyosarcoma as the second line of therapy.[8] The development of Yondelis® had to overcome major hurdles associated with low natural abundance and lengthy synthetic preparations.[9] One approach to solve the supply problem is the discovery of analogues that can be accessed via short synthetic procedures.[10]

Using this strategy, our studies of synthetic analogues of marine alkaloid rigidins A, B, C, D (Figure 1), isolated in minute amounts from the tunicate *Eudistoma cf. rigida* found near Okinawa and New Guinea,[11–14] revealed compounds with potent antiproliferative activities when the 7-deazaxanthine scaffold associated with the rigidins was replaced by the 7-deazahypoxanthine variant through the removal of the carbonyl at C2, such as in **1** and **2** (Figure 1).[15–18] These compounds resulted from systematic investigation of the rigidin-related scaffold **A** (top right corner in Figure 1) and they were found to target microtubule network in cancer cells.[15–18] Compound **2** also exhibited promising *in vivo* efficacy in a human colon cancer mouse model at doses as low as 2-3 mg/kg.[18] Compound **1** is accessible via a one-step multicomponent reaction from commercially available starting materials, whereas the synthesis of **2** was found to work best when it was split into two steps (Figure 1).[16–18] As a logical progression of this work, we explore here the analogues bearing substituents at positions *N*3 and *N*9 (Figure 1).

As part of preclinical evaluation of the rigidin-based anticancer agents, we also investigated their interaction with multi-drug resistance proteins. Often, tumors initially respond to chemotherapy but subsequently become refractory to the continuing treatment. Such resistance is known as “acquired” and it is commonly based on the development of a multi-drug resistant phenotype (MDR) impacting a wide range of structurally and mechanistically distinct antitumor agents.[19,20] MDR has plagued conventional cancer drug therapies, for example the widely used microtubule-disrupting agents such as the Vinca alkaloids[21] and taxanes.[22] Thus, we thoroughly evaluated whether our rigidin-based anticancer agents,

whose mode of action is also based on microtubule targeting, are capable of circumventing MDR mechanisms and can combat drug-resistant cancers.

Results and Discussion

Synthesis of *N*3- and *N*9-substituted 7-deazahypoxanthines

Although there are four potential nucleophilic sites in the deprotonated forms of **1** and **2**, namely *N*1, *N*3, *N*9 and *O*6, we found that these molecules react exclusively at *N*9. This finding was confirmed with an x-ray structure (Figure 2) of *N*9-*t*-butoxycarbonyl derivative of **1** (compound **3** in Scheme 1A) obtained by the treatment of **1** with NaH and $(Boc)_2O$.

Methylation of **3** at *N*3 and removal of the Boc group then furnished mono-methylated compound **5**. Alternatively, *N*9-methylated **6** was obtained by a direct reaction of **1** with NaH and MeI (Scheme 1A). *N*9-sulfonylated compound **9** was obtained by a different route involving a multicomponent condensation of benzaldehyde, malononitrile and sulfonamidoacetophenone **7** (Scheme 1B). The obtained pyrrole **8** was then cyclized by refluxing in formic acid, which was used as a solvent and reactant at the same time.

In our efforts to synthesize *N*-substituted analogues of **2**, we were able to obtain sulfonylated derivative **10** by a direct treatment of **2** with NaH and MsCl (Scheme 2). Compound **2** also gave *N*9-Boc derivative **11** when reacted with NaH and $(Boc)_2O$. Subsequent *N*3-methylation and removal of Boc then gave mono-methylated **12**. In contrast to direct methylation of **1**, similar conditions applied to **2** gave *N*3,*N*9-dimethyl derivative **14** along with expected **13**.

Structure-Activity Relationship studies

The synthesized analogues were evaluated for antiproliferative activities using the HeLa cell line as a model for human cervical adenocarcinoma and MCF-7 cells as a model for breast adenocarcinoma. The cells were treated with each compound for 48 h, and cell viability was assessed using the MTT method[23] (Table 1). We found that analogues containing single large substituents at *N*9 were equally or more potent than the original unsubstituted compounds. These included *N*9-*t*-butoxycarbonyl compounds **3** and **11** as well as *N*9-methylsulfonyl analogues **9** and **10**. In contrast, compounds containing a smaller *N*9 group, such as methyl in **6** and **13** were significantly less potent. Finally, the *N*3-substituted analogues **5**, **12** and **14** were totally inactive. In principle, these studies involving the variations in the *N*-substituents are consistent with our earlier SAR work, which showed that the modifications of the pyrimidine ring were not tolerated, whereas the pyrrole unit was a useful site for optimizing potency in this series of compounds. The present SAR results are similar between the **1**- and **2**-derived series of compounds indicating that the binding poses must be similar for C2-H or C2-alkyl structures.[18]

Inhibition of tubulin assembly

To exclude the possibility that the mode action was not inadvertently changed when the bulky substituents were added to the *N*9-position, the effects of these compounds on *in vitro* tubulin polymerization were evaluated.[24] In this assay, polymerization is monitored by the

increase of fluorescence due to the incorporation of a fluorescent reporter, 4',6-diamidino-2-phenylindole (DAPI), into growing microtubules. As a control, a known microtubule stabilizer paclitaxel induced potent enhancement of microtubule formation relative to the effect of the DMSO control (Figure 3A and B). Consistent with our previous results compounds **1** and **2** suppressed tubulin polymerization. In a similar manner, tubulin polymerization was inhibited by *N*9-*t*-butoxycarbonyl compounds **3** and **11** (Figure 3A and B), suggesting that the introduction of bulky groups at *N*9 of both **1** and **2** does not result in a change in mechanism of action.

Effects on microtubule organization in cells

Additional confirmation of tubulin targeting as the mechanism responsible for anticancer properties of the compounds in Table 1 came from studying their effects on the microtubule cytoskeleton in intact cells. To this end, cultured HeLa cells were treated with the original compounds **1** and **2** as well as their potent *N*9-substituted derivatives **3**, **9** and **11** at 50 nM, concentration relevant to their antiproliferative effects on HeLa cells (Table 1). Examination of interphase (Figure 4, top row) and mitotic (Figure 4, bottom row) cells revealed that while there were no pronounced effects on interphase microtubules, all compounds had marked effects on spindle morphology and chromosome alignment. While most cells established bipolar spindles, astral microtubules were frequently missing from one spindle pole, possibly due to the inherent asymmetries between centrosomes.[25] Most notably, treated cells invariably arrested in prometaphase with chromosomes clustered around the spindle poles, suggesting an inability to congress to the metaphase plate.

Examination of cells treated with compounds **2** and **11** over a range of doses revealed that effects on chromosome congression and spindle morphology were dose-dependent (Figure 5), with no noticeable effects on interphase microtubules, even at 100 nM (Figure 5B and C, top rows). In cells treated at concentrations near the GI_{50} (25 nM), overall spindle morphology was normal, but there were still chromosomes clustered at the spindle poles with syntelic attachments (Figure 5B and C, bottom rows). Syntelic chromosome attachments (where both sister chromatids are attached to the same spindle pole) activate the spindle assembly checkpoint, resulting in mitotic arrest and eventual cell death.[26] In light of the minimal effects on interphase microtubules (Figures 4 and 5) and the known requirement of microtubule dynamics for proper spindle assembly, chromosome alignment and segregation,[27] it is likely that the observed effects on growth inhibition are due to inability of treated cells to establish proper bioriented chromosome attachments at the metaphase plate rather than a gross disruption of the mitotic spindle.

Interaction with multi-drug resistance proteins

As mentioned in the introduction, "acquired" resistance is commonly based on the development of an MDR phenotype impacting a wide range of structurally and mechanistically distinct antitumor agents. This type of resistance is frequently mediated by MDR proteins belonging to the vast superfamily of ABC transporters.[19,20] Due to their ubiquitous tissue and organ distribution and extremely low specificity, they are able to prevent many substances from entering the target cell. Moreover, they play an important role in constituting the biochemical base of epithelial barriers, thus protecting vital organs

located behind such barriers (e.g. brain, testes or fetal organs) against drugs or other xenobiotics. Major drug regulatory agencies, e.g. the Food and Drug Administration, or European Medicines Agency, require that the role of major MDR proteins be taken into account. Thus, we assessed the potential role of ABCB1 (known also as MDR1 or Pgp), ABCC1 (known also as MRP1) and ABCG2 (known also as BCRP) in conferring resistance to rigidin analogues as well as potential modulatory effects of rigidin derivatives on selected MDR proteins.

First, we studied whether the cytotoxic effects of the rigidin analogues depended on different MDR protein profiles. We chose to work with colon cancer cells, as compound **2** showed highly promising results in earlier *in vivo* experiments involving a colon cancer xenograft model[18] and a panel of drug-resistant daughter lines of SW620 (human colorectal adenocarcinoma) cells were obtained in our laboratories previously.[28] Specifically, SW620C cells overexpress ABCG2; SW620E and SW620M cell lines are characterized by overexpression of ABCC; SW620D, SW620E, and SW620V cells exhibit high expression levels of ABCB1. We also included MDCKII (canine renal epithelium) cell line and *hABCG2*- and *hABCB1*-transfected sublines (MDCKII-BCRP and MDCKII-MDR1, respectively), to determine whether the two cell sets of different origin and basic metabolic activity display different sensitivities to the rigidin analogues.

Analysis of results obtained with the neutral red accumulation assay[29] and presented in Table 2 and Table 3 reveals that none of MDR proteins confers resistance to both the parent compounds **1** and **2** as well as their *N*9-*t*-butoxycarbonyl derivatives **3** and **11**. Toxicity of these substances is generally lower for SW620 cells (in ten to hundred nanomolar range, Table 2) than for MDCKII cells (between 14 and 24 nM, Table 3). The SW620 and ABCC1-overexpressing SW620M cell lines appear to be more sensitive to compound **11** than other lines, which could suggest some involvement of ABCB1 in its detoxication as virtually no ABCB1 is expressed in this cell line. However, no such tendency is seen in the MDCKII panel.

Despite negative results of cytotoxicity assay, we proceeded to determine if the rigidin analogues added at a low and virtually non-toxic concentration (10 nM) were able to modulate a well-defined resistance to some model cytotoxic drugs. We chose mitoxantrone as a model substrate for human ABCG2[30] and vincristine as a model substrate for ABCB1.[31] The resistance factors (IC_{50} ratio for resistant and sensitive cells for a given drug) observed in our system for these drugs were 8 for mitoxantrone and ABCG2 and 38 for vincristine and ABCB1 (see Table 4). If sensitizing effects (i.e., significant reduction of resistance factor) were observed, it would suggest direct interactions of rigidin derivatives with MDR proteins. However, as seen in Table 4, no such results were detected. 10 μM verapamil (Ver) and 10 μM Ko143 were used as positive controls (both compounds are specific inhibitors of ABCB1 and ABCG2, respectively). Values observed for investigated rigidin analogues did not differ significantly from controls (the confidence intervals fairly overlapped). Therefore, it can be induced that rigidins do not exert any long-term effects on MDR protein expression or function.

As it is possible that rigidin analogues undergo conversion to metabolites that do not interact with MDR proteins, we finally determined whether there is any direct interaction between investigated compounds and transporters in a real-time transport assay.[32] We employed three different assays specific for a given protein of interest – calcein accumulation assay for determination of ABCB1 activity,[33] modified BCECF extrusion assay[34] for ABCC1 assessment and pheophorbide *a* accumulation to measure ABCG2 function[35] (Table 5). In this case, despite Ver and Ko143 as inhibitors of ABCB1 and ABCG2, respectively, MK571 was used as a specific inhibitor of ABCC1. As evident from Table 5, no direct interaction between investigated rigidin analogues and MDR proteins exists, as none of the compounds is able to inhibit transporter activity even partially. Summing up all results presented in Tables 2 – 5, rigidins exhibit no modulatory activity on MDR protein function. Taking into account also their antiproliferative properties, they can be considered agents of possibly great therapeutic potential as they pose no risk of development of classical multidrug resistance.

Conclusion

Previous work with the synthetic analogues of marine alkaloid rigidins, involving promising *in vitro* and *in vivo* data, revealed the potential of these compounds as anticancer agents. While various parts of this 7-deazahypoxanthine skeleton had been investigated to derive SAR data, the *N*3- and *N*9-positions remained unexplored. As reported herein, we developed synthetic chemistry to derivatize both nitrogens separately. The derivatization at *N*9 led to compounds with retained activities and the antitubulin mode of action of the original *N*3- and *N*9-unsubstituted compounds. Position *N*9 is thus identified as a site that can be utilized to optimize the properties of these compounds in further preclinical work.

Work reported herein also demonstrated that MDR proteins do not confer resistance to the previously investigated *N*3- and *N*9-unsubstituted compounds as well as their new *N*9-*t*-butoxycarbonyl derivatives. Moreover, no direct interaction of these compounds with any of the transporters tested was demonstrated, either in short-term or long-term assays. It can thus be postulated that the investigated rigidin analogues are promising cytotoxic agents that are able to cross epithelial barriers guarded by multidrug resistance transporters.

Experimental Section

Chemistry

General: All reagents, solvents and catalysts were purchased from commercial sources (Acros Organics and Sigma-Aldrich) and used without purification. All reactions were performed in oven-dried flasks open to the atmosphere or under nitrogen and monitored by thin layer chromatography (TLC) on TLC precoated (250 μm) silica gel 60 F254 glass-backed plates (EMD Chemicals Inc.). Visualization was accomplished with UV light. Flash column chromatography was performed on silica gel (32-63 μm, 60 Å pore size). ^{1}H and ^{13}C NMR spectra were recorded on a Bruker 400 spectrometer. Chemical shifts (δ) are reported in ppm relative to the TMS internal standard. Abbreviations are as follows: s (singlet), d (doublet), t (triplet), q (quartet), m (multiplet). HRMS analyses were performed using Waters Synapt G2 LCMS.

***tert*-Butyl 6-benzoyl-4-oxo-5-phenyl-1,4-dihydro-7*H*-pyrrolo[2,3-*d*]pyrimidine-7-carboxylate (3):** To a solution of **1**[15] (35.0 mg, 0.111 mmol) in DMF (1 mL) was added NaH (60%) (6.6 mg, 0.17 mmol) at 0 °C and stirred for 15 minutes. To that $(Boc)_2O$ (35.7 μL, 0.155 mmol) and DMAP (2.7 mg, 0.022 mmol) were added at 0 °C. The resultant mixture was allowed to warm up to room temperature and stirred for 4 h. After completion, the reaction was quenched with saturated NH_4Cl and then extracted with ethyl acetate. The organic layer was washed with water and dried over anhydrous Na_2SO_4 and then concentrated to give crude residue. The crude product was purified by column chromatography using 2.5% MeOH/DCM solvent system and the product was obtained in 73% yield (33.7 mg). ^{1}H NMR (500 MHz, DMSO-*d*6) δ 12.49 (s, 1H), 8.18 (d, *J* = 2.8 Hz, 1H), 7.64 (dd, *J* = 8.3, 1.2 Hz, 2H), 7.56 – 7.50 (m, 1H), 7.40 – 7.35 (m, 2H), 7.30 – 7.25 (m, 2H), 7.20 – 7.15 (m, 3H), 1.26 (s, 9H). ^{13}C NMR (126 MHz, DMSO) δ 187.4, 157.8, 149.3, 147.8, 146.2, 136.8, 133.5, 130.4 (2C), 128.9 (2C), 128.6 (2C), 128.0, 127.5, 127.2 (2C), 125.1, 107.2, 85.9, 79.1, 26.7 (3C). HRMS (ESI) calcd for $C_{24}H_{22}N_3O_4$ (M+H) 416.1610, found 416.1611.

***tert*-Butyl 6-benzoyl-1-methyl-4-oxo-5-phenyl-1,4-dihydro-7*H*-pyrrolo[2,3-*d*]pyrimidine-7-carboxylate (4):** To a solution of **3** (15.0 mg, 0.036 mmol) in DMF (1.5 mL) was added NaH (60%) (1.9 mg, 0.047 mmol) at 0 °C and stirred for 10 minutes. To that MeI (2.6 μL, 0.043 mmol) was added at 0 °C. The resultant mixture was allowed to warm up to rt and stirred for 2 h. After completion, the reaction was quenched with ice and then extracted with ethyl acetate. The organic layer was washed with water and dried over anhydrous Na_2SO_4 and then concentrated to give crude residue. The crude product was purified by preparative TLC using 2.0% MeOH/DCM solvent system and the product was obtained in 65% yield (10.0 mg). ^{1}H NMR (500 MHz, CD_3OD) δ 8.36 (s, 1H), 7.73 – 7.69 (m, 2H), 7.50 – 7.46 (m, 1H), 7.35 – 7.29 (m, 4H), 7.17 – 7.13 (m, 3H), 3.58 (s, 3H), 1.33 (s, 9H). ^{13}C NMR (125 MHz, DMSO-d6) δ 187.4, 157.4, 150.5, 148.7, 146.1, 136.8, 133.6, 130.3 (2C), 128.9 (2C), 128.6 (2C), 128.3, 127.5, 127.2 (2C), 124.8, 106.4, 85.9, 79.2, 33.5, 26.7 (3C). HRMS (ESI) calcd for $C_{25}H_{23}N_3NaO_4$ (M+Na) 452.1586, found 452.1588.

6-Benzoyl-1-methyl-5-phenyl-1,7-dihydro-4*H*-pyrrolo[2,3-*d*]pyrimidin-4-one (5): To a solution of **4** (8.0 mg, 0.018 mmol) in DCM (1.5 mL) was added 100 μL of TFA at 0 °C and stirred for 10 min. The resultant mixture was allowed to warm up rt and stirred for 2 h. After completion, the reaction was diluted with hexanes, co-distilled with toluene to obtain the product in 97% yield (5.9 mg). ^{1}H NMR (500 MHz, DMSO-*d*6) δ 12.76 (s, 1H), 8.35 (s, 1H), 7.45 – 7.41 (m, 2H), 7.35 – 7.30 (m, 1H), 7.19 – 7.11 (m, 4H), 7.06 – 7.00 (m, 3H), 3.43 (s, 3H). ^{13}C NMR (125 MHz, DMSO-d6) δ 187.8, 158.2, 149.7, 148.9, 137.4, 131.9, 131.1 (2C), 129.1 (2C), 127.9, 127.7 (2C), 126.8 (2C), 126.7 (2C), 126.5, 105.5, 99.5, 33.2. HRMS (ESI) calcd for $C_{20}H_{16}N_3O_2$ (M+H) 330.1242, found 330.1242.

6-Benzoyl-7-methyl-5-phenyl-1,7-dihydro-4*H*-pyrrolo[2,3-*d*]pyrimidin-4-one (6): To a solution of **1**[15] (6.0 mg, 0.019 mmol) in DMF (1.5 mL) was added NaH (60%) (1.0 mg, 0.024 mmol) at 0 °C and stirred for 10 minutes. To that MeI (1.4 μL, 0.022 mmol) was added at 0 °C. The resultant mixture was allowed to warm up to rt and stirred for 2 hours. After completion, the reaction was quenched with ice and then extracted with ethyl acetate.

The organic layer was washed with water and dried over anhydrous Na_2SO_4 and then concentrated to give crude residue. The crude product was purified by preparative TLC using 3.0% MeOH/DCM solvent system and the product was obtained in 57% yield (3.6 mg). ^{1}H NMR (500 MHz, $CDCl_3$) δ 11.40 (s, 1H), 7.86 (s, 1H), 7.62 – 7.56 (m, 2H), 7.31 – 7.27 (m, 3H), 7.14 – 7.04 (m, 5H), 3.97 (s, 3H). ^{13}C NMR (125 MHz, $CDCl_3$) δ 189.5, 160.2, 149.8, 144.6, 137.6, 132.7, 132.0, 131.1 (2C), 129.9 (2C), 129.8, 127.9 (2C), 127.4 (2C), 127.3, 126.8, 105.5, 31.0. HRMS (ESI) calcd for $C_{20}H_{16}N_3O_2$ (M+H) 330.1242, found 330.1238.

2-Amino-5-benzoyl-1-(methylsulfonyl)-4-phenyl-1H-pyrrole-3-carbonitrile (8): To a stirred solution of *N*-methyl sulfonamidoacetophenone (0.2 mmol), benzaldehyde (0.26 mmol) and malononitrile (0.26 mmol) in acetonitrile (3 mL) was added Et_3N (0.073 mmol). The mixture was refluxed until the starting sulfonamide disappeared (TLC). After this time the reaction mixture was cooled to rt and DDQ (0.6 mmol) was added under the nitrogen atmosphere. The reaction mixture was stirred at rt for 6 h. The crude product was concentrated and purified by column chromatography using 1:40 EtOAc/DCM solvent system and the product was obtained in 52% yield (38 mg). ^{1}H NMR (400 MHz, acetone-*d*6) δ 7.68 (d, *J* = 8.4 Hz, 2H), 7.38 – 7.34 (m, 1H), 7.23 – 7.14 (m, 7H), 6.90 (s, 2H), 3.95 (s, 3H); ^{13}C NMR (100 MHz, aceton-d6) δ 186.2, 137.8, 133.5, 132.7, 131.0, 129.7 (2C), 129.3, 129.1 (2C), 128.3, 128.2 (2C), 128.0, 127.9 (2C), 122.2, 114.1, 43.1. HRMS (ESI) calcd for $C_{19}H_{16}N_3O_3S$ (M+H) 366.0912, found 366.0917.

6-Benzoyl-7-(methylsulfonyl)-5-phenyl-1,7-dihydro-4*H*-pyrrolo[2,3-*d*]pyrimidin-4-one (9): To compound **8** (0.1 mmol), was added formic acid (4 mL) and the mixture was refluxed under nitrogen atmosphere for 6 h. The formation of the compound **9** was monitored by TLC. After compound **8** disappeared, the mixture was cooled to rt and the crude product was purified by preparative TLC using 1:2 EtOAc/hexanes solvent system and the product was obtained in 21% yield (8.0 mg). ^{1}H NMR (400 MHz, acetone-*d*6) δ 11.45 (s, 1H), 8.29 (s, 1H), 7.79 (d, *J* = 7.2Hz, 2H), 7.56 – 7.52 (m, 1H), 7.41 – 7.40 (m, 4H), 7.21–7.20 (m, 3H), 3.75 (s, 3H); ^{13}C NMR (100 MHz, aceton-d6) δ 187.9, 157.2, 149.8, 147.0, 137.8, 133.4, 130.6, 130.4 (2C), 129.2 (2C), 128.5 (2C), 127.6 (2C), 127.3 (2C), 124.1, 108.7, 43.0. HRMS (ESI) calcd for $C_{20}H_{15}N_3O_4SNa$ (M+Na) 416.0681, found 416.0680.

6-Benzoyl-7-(methylsulfonyl)-2-(pent-4-yn-1-yl)-5-phenyl-1,7-dihydro-4*H*-pyrrolo[2,3-*d*]pyrimidin-4-one (10): To a solution of **2**[18] (20.0 mg, 0.052 mmol) in DMF (1.0 mL) was added NaH (60%) (3.1 mg, 0.078 mmol) at 0 °C and stirred for 10 minutes. To that MsCl (5.6 μL, 0.073 mmol) and DMAP (1.2 mg, 0.010 mmol) were added at 0 °C. The resultant mixture was heated at 70 °C and stirred for 24 h. The reaction was quenched with ice and then extracted with ethyl acetate, organic layer was washed with water, dried over anhydrous Na_2SO_4 and then concentrated to give crude residue. The crude product was purified by preparative TLC using 2.5% MeOH/DCM solvent system, resulting in recovered **2** (14 mg) and obtained **10** in 46% yield (3.3 mg of product from 6 mg of **2**). ^{1}H NMR (500 MHz, DMSO) δ 12.55 (s, 1H), 7.72 – 7.65 (m, 2H), 7.59 – 7.52 (m, 1H), 7.46 – 7.39 (m, 2H), 7.32 – 7.27 (m, 2H), 7.24 – 7.18 (m, 3H), 3.73 (s, 3H), 2.89 – 2.76 (m, 3H),

2.38 – 2.29 (m, 2H), 2.02 – 1.89 (m, 2H). ^{13}C NMR (125 MHz, DMSO) δ 187.7, 159.9, 158.2, 149.7, 137.4, 133.6, 130.3, 130.0 (2C), 128.9 (2C), 128.7 (2C), 127.6, 127.4 (2C), 127.2, 123.6, 105.9, 83.8, 71.8, 43.2, 32.6, 25.2, 17.0. HRMS (ESI) calcd for $C_{25}H_{22}N_3O_4S$ (M+H) 460.1331, found 460.1334.

***tert*-Butyl 6-benzoyl-4-oxo-2-(pent-4-yn-1-yl)-5-phenyl-1,4-dihydro-7*H*-pyrrolo[2,3-*d*]pyrimidine-7-carboxylate (11):** To a solution of **2**[18] (50.0 mg, 0.131 mmol) in DMF (2 mL) was added NaH (60%) (7.8 mg, 0.20 mmol) at 0 °C and stirred for 15 minutes. To that $(Boc)_2O$ (45.1 μL, 0.196 mmol) and DMAP (3.2 mg, 0.026 mmol) were added at 0 °C. The resultant mixture was allowed to warm up to rt and stirred for 4 h. After completion, the reaction was quenched with saturated NH_4Cl and then extracted with ethyl acetate. The organic layer was washed with water and dried over anhydrous Na_2SO_4 and then concentrated to give crude residue. The crude product was purified by column chromatography using 2.0% MeOH/DCM solvent system and the product was obtained in 78% yield (4.9 mg). ^{1}H NMR (500 MHz, $CDCl_3$) δ 12.31 (s, 1H), 7.74 – 7.70 (m, 2H), 7.45 – 7.38 (m, 3H), 7.32 – 7.25 (m, 2H), 7.23 – 7.17 (m, 3H), 2.85 – 2.81 (m, 2H), 2.24 (td, *J* = 7.0, 2.6 Hz, 2H), 2.07 – 2.00 (m, 2H), 1.96 (t, *J* = 2.6 Hz, 1H), 1.38 (s, 9H). ^{13}C NMR (125 MHz, DMSO-d6) δ 187.3, 159.9, 158.6, 149.6, 146.7, 137.0, 133.3, 130.4 (2C), 128.8 (2C), 128.5 (2C), 127.6, 127.4, 127.2 (2C), 125.4, 105.2, 85.6, 83.9, 71.7, 54.9, 32.7, 26.9 (3C), 25.1, 17.2. HRMS (ESI) calcd for $C_{29}H_{28}N_3O_4$ (M+H) 482.2080, found 482.2077.

6-Benzoyl-1-methyl-2-(pent-4-yn-1-yl)-5-phenyl-1,7-dihydro-4*H*-pyrrolo[2,3-*d*]pyrimidin-4-one (12): To a solution of **11** (10.0 mg, 0.021 mmol) in DMF (1.5 mL) was added NaH (60%) (1.1 mg, 0.027 mmol) at 0 °C and the mixture was stirred for 10 min. To the mixture was added MeI (1.6 μL, 0.025 mmol) at 0 °C. The resultant mixture was allowed to warm up to rt and stirred for 3 h. After completion, the reaction was quenched with ice and then extracted with ethyl acetate. The organic layer was washed with water, dried over anhydrous Na_2SO_4 and then concentrated to give *N*9-Boc-*N*3-methylated compound in 69% yield (7.1 mg). It was used for the boc-deprotection reaction without further purification. To a solution of *N*9-boc-*N*3-methylated compound (5.0 mg, 0.010 mmol) in DCM (1.5 mL) was added 100 μL of TFA at 0 °C and stirred for 10 min. The resultant mixture was allowed to warm up to rt and stirred for 2 h. After completion, the reaction was diluted with DCM, washed with saturated $NaHCO_3$ solution and H_2O. The organic layer was dried over anhydrous Na_2SO_4 and then concentrated to give crude residue. The crude product was purified by preparative TLC using 2.0% MeOH/$CHCl_3$ solvent system and to obtain **12** in 55% yield (2.1 mg). ^{1}H NMR (500 MHz, DMSO-*d*6) δ 12.57 (s, 1H), 7.44 – 7.40 (m, 2H), 7.34 – 7.30 (m, 1H), 7.19 – 7.11 (m, 4H), 7.07 – 7.00 (m, 3H), 3.00 – 2.92 (m, 2H), 2.85 (t, *J* = 2.6 Hz, 1H), 2.37 (td, *J* = 7.1, 2.6 Hz, 2H), 2.02 – 1.93 (m, 2H); ^{13}C NMR (125 MHz, DMSO-d6) δ 187.6, 159.1, 158.7, 147.8, 137.5, 132.5, 131.8, 131.1 (2C), 129.0 (2C), 127.7 (2C), 127.5, 126.7 (2C), 126.63, 126.61, 103.6, 84.1, 71.8, 33.5, 29.3, 24.9, 17.3. HRMS (ESI) calcd for $C_{25}H_{21}N_3NaO_2$ (M+Na) 418.1531, found 418.1536.

6-Benzoyl-7-methyl-2-(pent-4-yn-1-yl)-5-phenyl-1,7-dihydro-4*H*-pyrrolo[2,3-*d*]pyrimidin-4-one (13) and 6-benzoyl-1,7-dimethyl-2-(pent-4-yn-1-yl)-5-

phenyl-1,7-dihydro-4*H*-pyrrolo[2,3-*d*]pyrimidin-4-one (14): To a solution of **2**[18] (10.0 mg, 0.026 mmol) in DMF (1.0 mL) was added NaH (60%) (1.3 mg, 0.034 mmol) at 0 °C and stirred for 10 min. To that MeI (1.9 μL, 0.031 mmol) was added at 0 °C. The resultant mixture was allowed to warm up to rt and stirred for 3 h. After completion, the reaction was quenched with ice and then extracted with ethyl acetate. The organic layer was washed with water and dried over anhydrous Na_2SO_4 and then concentrated to give crude residue. The crude product was purified by preparative TLC using 3.0% MeOH/$CHCl_3$ solvent system resulting in two compounds **13** in 56% (5.8 mg) and **14** in 23% (2.5 mg). Compound **13**: ^{1}H NMR (500 MHz, DMSO-*d*6) δ 12.03 (s, 1H), 7.52 – 7.49 (m, 2H), 7.35 – 7.31 (m, 1H), 7.18 – 7.13 (m, 4H), 7.03 – 6.99 (m, 3H), 3.81 (s, 3H), 2.85 (t, *J* = 2.6 Hz, 1H), 2.78 – 2.73 (m, 2H), 2.30 (td, *J* = 7.1, 2.6 Hz, 2H), 1.98 – 1.91 (m, 2H); ^{13}C NMR (125 MHz, DMSO-d6) δ 188.7, 159.0, 158.5, 149.7, 137.7, 132.5, 132.3, 130.9 (2C), 129.5 (2C), 128.4, 127.8 (2C), 126.9 (2C), 126.7, 125.9, 103.0, 83.8, 71.8, 32.9, 30.5, 25.6, 17.3. HRMS (ESI) calcd for $C_{25}H_{21}N_3NaO_2$ (M+Na) 418.1531, found 418.1530. Compound **14**: ^{1}H NMR (500 MHz, DMSO-*d*6) δ 7.53 – 7.49 (m, 2H), 7.36 – 7.31 (m, 1H), 7.18 – 7.13 (m, 4H), 7.04 – 6.99 (m, 3H), 3.82 (s, 3H), 3.48 (s, 3H), 3.01 – 2.96 (m, 2H), 2.85 (t, *J* = 2.6 Hz, 1H), 2.40 (td, *J* = 7.1, 2.6 Hz, 2H), 2.06 – 1.98 (m, 2H); ^{13}C NMR (125 MHz, DMSO) δ 188.7, 158.8, 158.4, 147.7, 137.6, 132.5, 132.2, 130.9 (2C), 129.5 (2C), 128.7, 127.8 (2C), 126.8 (2C), 126.7, 125.8, 102.1, 84.1, 71.8, 33.4, 30.2, 29.4, 24.7, 17.2. HRMS (ESI) calcd for $C_{26}H_{24}N_3O_2$ (M+H) 410.1869, found 410.1871.

Biology

Cell culture: Human cancer cell lines were obtained from the American Type Culture Collection (ATCC, Manassas, VA, USA). The HeLa (ATCC CCL-2) and MCF-7 (ATCC HTB-22) cells were cultured in RPMI media supplemented with 10% heat-inactivated fetal calf serum (FCS), 4 mM L-glutamine, 100 mg/mL gentamicin, 200 U/mL penicillin, and 200 mg/mL streptomycin. These cell lines were maintained and grown at 37 ºC, 95% humidity, 5% CO_2. SW620 (human colorectal adenocarcinoma) and a panel of drug-resistant daughter lines were obtained as described elsewhere,[28] while MDCKII (canine renal epithelium) and *hABCG2*- and *hABCB1*-transfected sublines (MDCKII-BCRP and MDCKII-MDR1, respectively) were purchased from Solvo (Solvo Biotechnology, Szeged, Hungary). These cell lines were cultured in standard cell culture conditions (37 °C, 5% CO_2, 95% relative humidity) in high-glucose Dulbecco's Modified Eagle Medium buffered with HEPES, supplemented with Glutamax-I and 10% v/v fetal bovine serum (Thermo Fisher Scientific Inc., Waltham, MA USA). Care was taken to avoid cross-contamination between the cell lines. The cells were tested every 3 months for *Mycoplasma* contamination with a MycoProbe® Mycoplasma Detection Kit by R&D (Minneapolis, Minnesota, USA).

Antiproliferative Properties:

MTT assay (Table 1): The cells were prepared by trypsinizing each cell line and seeding 4 × 10^3 cells per well into microtiter plates. All compounds were dissolved in DMSO at a concentration of either 100 mM or 25 mM prior to cell treatment. The cells were grown for 24 h before treatment at concentrations ranging from 0.004 to 100 μM and incubated for 48 h in 200 μL media. 20 μL of MTT reagent in serum free medium (5 mg/mL) was added to each well and incubated further for 2 h. Media was removed, and the resulting formazan

crystals were re-solubilized in 100 μL of DMSO. A_{490} was measured using a Thermomax Molecular Device plate reader. Cells treated with 0.1% DMSO were used as a control.

Neutral red accumulation assay (Tables 2, 3, 4): Cells suspended in 100 μL of a complete medium were seeded on 96-well plates at a density of 10^4/well. The cells were allowed to attach for 24 h and then the investigated substance was added at the desired concentration. Stock solutions were prepared in DMSO and the solvent concentration was maintained constant in all wells, including the controls. The final DMSO concentration did not exceed 0.1% v/v and was determined to be non-toxic to the cells. After 70 h of incubation, neutral red was added to the medium to a final concentration of 1.15 mM. After further 2 h, the medium was removed, the plate was rinsed twice with phosphate-buffered saline and 200 mm^3 of 16.65 mM acetic acid in 50% v/v ethanol were added to solubilize the cells. The absorbance was measured at 540 nm analytic wavelength and 690 nm reference wavelength. The results were turned into percentage of controls and the GI_{50} values for each cell line and substance were calculated with the GraphPad Prism 5.02 software (GraphPad Inc.) using a four-parameter nonlinear logistic regression.

Transport assays: Drug-resistant variants of SW620 cells expressing elevated number of ABCB1 (SW620V), ABCC1 (SW620M) or ABCG2 (SW620C) protein copies were trypsinized and suspended in a complete cell culture medium pre-warmed to 37 °C at a final density of approx. 1×10^6/mL. Tested compounds were added from DMSO stock solutions to a final concentration of 1 μM. Respective samples were supplemented with a specific fluorescent marker (calcein-AM for ABCB1, BCECF-AM for ABCC1 and pheophorbide *a* for ABCG2) at 100 nM final concentration. For control, given protein-specific inhibitors (10 μM verapamil for ABCB1, 25 μM MK571 for ABCC1 and 10 μM Ko143 for ABCG2) were added to parallel, tested compound-free, samples. For ABCB1 and ABCG2 assays (dye accumulation assays), intracellular fluorescence was measured immediately after dye addition (time 0) and every 3–5 minutes up to approx. 30 minutes using a flow cytometer (LSRII, Becton Dickinson, East Rutherford, NJ, USA) set at 488 nm excitation and 530/30 emission for calcein/ABCB1 assay and 405 nm excitation and 655/8 nm emission for pheophorbide a/ABCG2 assay. For BCECF/ABCC1 assay (dye exclusion assay), the sample was preincubated for 10 minutes at 37°C, then centrifuged (100×g, 10', 4°C) and re-suspended in a fresh medium. Intracellular BCECF concentration was then immediately measured at 488 nm excitation and 530/30 emission (time 0). Further measurements were performed in 15-minute intervals. All samples were incubated at 37°C between measurements. Accumulation/exclusion curves were plotted and accumulation rate or dye half-life as a measure of its cytoplasmic retention were assessed with the GraphPad Prism 5.02 software (GraphPad Inc.).

***In Vitro* Tubulin Polymerization Assay:** To investigate whether the test compound bound and inhibited polymerization of tubulin, experiments were performed with the tubulin polymerization assay obtained from Cytoskeleton, Inc. A 10x stock solution of a test compound was prepared using ultrapure water. The tubulin reaction mix was prepared by mixing 243 μL of buffer 1 [80 mM PIPES sequisodium salt; 2.0 mM $MgCl_2$; 0.5 mM ethylene glycol-bis(2-aminoethyl ether)-*N*,*N*,*N*',*N*'-tetraacetic acid, pH 6.9, 10 μM DAPI],

112 μL tubulin glycerol buffer [80 mM PIPES sequisodium salt; 2.0 mM $MgCl_2$; 0.5 mM ethylene glycol-bis(2-aminoethyl ether)-*N*,*N*,*N*′,*N*′-tetraacetic acid, 60% v/v glycerol, pH 6.9], 1 mM GTP (final concentration), and 2 mg/mL tubulin protein (final concentration). The reaction mixture was kept on ice and used within an hour of preparation. The 10x test compounds were pipetted into the corresponding wells and warmed in the plate reader for 1 min, after which time they were diluted with the reaction mixture to their final 1x concentrations and placed in the plate reader. The test compounds were incubated with the tubulin reaction mixture at 37 °C. The effect of each agent on tubulin polymerization was monitored in a temperature-controlled BioTek Synergy H4 Hybrid Multi-Mode Fluorescence, Absorbance and Luminescence Microplate Reader for one hour, with readings acquired every 60 s.

Morphological Analysis of Microtubule Organization in HeLa Cells: HeLa cells were incubated in the absence or presence of a test compound for 4 h prior to fixation with 3.7% formaldehyde in phosphate-buffered saline (PBS) and permeabilization in 0.1% Triton X-100 in PBS. Cells were then briefly blocked with 3% Bovine Serum Albumin in PBS, and then probed with antibodies specific for tubulin (Sigma, St. Louis, MO) and the centromere marker CENP-B (Abcam, Cambridge, MA). Hoescht 33342 (Life Technologies) was included to highlight DNA. Samples were imaged using a Leica TCS-SP5 II confocal microscope at the Core University Research Resources Laboratory at New Mexico State University, and figures were prepared using Adobe Photoshop CS5.

Supplementary Material

Refer to Web version on PubMed Central for supplementary material.

Acknowledgments

This project was supported by the grant from the National Cancer Institute (CA186046-01A1). SR and LF acknowledge their NMT Presidential Research Support. RMK and CBS acknowledge support from the Cowboys for Cancer Research. WvO and AvdW thank the National Research Foundation (NRF)-South Africa for support in terms of CPRR (113322) and postgraduate research funding respectively.

References

[1]. Urban S, Hickford SJH, Blunt JW, Munro MHG, Curr. Org. Chem 2000, 4, 765–807.

[2]. Hill RA, Annu. Rep. Prog. Chem., Sect. B, 2005, 101, 124–136.

[3]. Simmons TL, Andrianasolo E, McPhail K, Flatt P, Gerwick WH, Mol. Cancer Ther 2005, 4, 333–342. [PubMed: 15713904]

[4]. Dembitsky VM, Gloriozova TA, Poroikov VV, Mini-Rev. Med. Chem 2005, 5, 319–336. [PubMed: 15777266]

[5]. Petek BJ, Loggers ET, Pollack SM, Jones RL, Mar. Drugs 2015, 13, 974–983. [PubMed: 25686274]

[6]. Mascilini F, Amadio G, Di Stefano MG, Ludovici M, Di Legge A, Conte C, De Vincenzo R, Ricci C, Mascuillo V, Salutari V, Scambia G, Ferrandina G, Onco Targ. Ther 2014, 7, 1273–1284.

[7]. Mabuchi S, Hisamatsu T, Kawase C, Hayashi M, Sawada K, Mimura K, Takahashi K, Takahashi T, Kurachi H, Kimura T, Clin. Cancer Res 2011, 17, 4462–4473. [PubMed: 21622721]

[8]. Barone A, Chi DC, Theoret MR, Chen H, He K, Kufrin D, Helms WS, Subramaniam S, Zhao H, Patel A, Goldberg KB, Keegan P, Pazdur R, Clin. Cancer Res 2017, 23, 7448–7453. [PubMed: 28774898]

[9]. Cuevas C, Francesch A, Nat. Prod. Rep 2009, 26, 322–337. [PubMed: 19240944]

[10]. Gomes NGM, Dasari R, Chandra S, Kiss R, Kornienko A, Mar. Drugs 2016, 14, 98.

[11]. Kobayashi J, Cheng J, Kikuchi Y, Ishibashi M, Yamamura S, Ohizumi Y, Ohta T, Nozoec S, Tetrahedron Lett. 1990, 31, 4617–4620.

[12]. Tsuda M, Nozawa K, Shimbo K, Kobayashi J, J. Nat. Prod 2003, 66, 292–294. [PubMed: 12608870]

[13]. Davis RA, Christensen LV, Richardson AD, Moreira da Rocha R, Ireland CM, Mar. Drugs 2003, 1, 27–33.

[14]. Frolova LV, Evdokimov NM, Hayden K, Malik I, Rogelj S, Kornienko A, Magedov IV, Org. Lett 2011, 13, 1118–1121. [PubMed: 21268660]

[15]. Frolova LV, Magedov IV, Romero A, Karki M, Otero I, Hayden K, Evdokimov NM, Banuls LMY, Rastogi SK, Smith WR, Lu SL, Kiss R, Shuster CB, Hamel E, Betancourt T, Rogelj S, Kornienko A, J. Med. Chem 2013, 56, 6886–6900. [PubMed: 23927793]

[16]. Scott R, Karki M, Reisenauer MR, Rodrigues R, Dasari R, Smith WR, Pelly SC, van Otterlo WAL, Shuster CB, Rogelj S, Magedov IV, Frolova LV, Kornienko A, ChemMedChem. 2014, 9, 1428–1435. [PubMed: 24644272]

[17]. Dasari R, Kornienko A, Chem. Heterocycl. Compd 2014, 50, 139–144.

[18]. Medellin DC, Zhou Q, Scott R, Hill RM, Frail SK, Dasari R, Ontiveros SJ, Pelly SC, van Otterlo WAL, Betancourt TB, Shuster CB, Hamel E, Bai R, LaBarbera DV, Rogelj S, Frolova LV, Kornienko A, J. Med. Chem 2016, 59, 480–485. [PubMed: 26641132]

[19]. Gottesman MM, Fojo T, Bates SE, Nat. Rev. Cancer 2002, 2, 48–58. [PubMed: 11902585]

[20]. Saraswathy M, Gong SQ, Biotechnol. Adv 2013, 31, 1397–1407. [PubMed: 23800690]

[21]. Chen GK, Duran GE, Mangili A, Beketic-Oreskovic L, Sikic BI, Br. J. Cancer 2000, 83, 892–898. [PubMed: 10970691]

[22]. Geney R, Ungureanu M, Li D, Ojima I, Clin. Chem. Lab. Med 2002, 40, 918–925. [PubMed: 12435109]

[23]. Mosmann T, Immunol J. Methods 1983, 65, 55–63.

[24]. Jordan MA, Wilson L, Nature Rev. Cancer 2004, 4, 253–265. [PubMed: 15057285]

[25]. Pelletier L, Yamashita YM, Curr. Opin. Cell Biol 2012, 24, 541–546. [PubMed: 22683192]

[26]. Lischetti T, Nilsson J, Mol. Cell Oncol 2015, 2, e970484. [PubMed: 27308407]

[27]. Wittmann T, Hyman A, Desai A, Nat. Cell Biol 2001, 3, E28–34. [PubMed: 11146647]

[28]. Błauż A, Rychlik B, J. Pharmacol. Toxicol. Methods 2017, 84, 57–65. [PubMed: 27838457]

[29]. Borenfreund E, Puerner JA, Toxicol. Lett 1985, 24, 119–124. [PubMed: 3983963]

[30]. Doyle LA, Yang W, Abruzzo LV, Krogmann T, Gao Y, Rishi AK, Ross DD, Proc. Natl. Acad. Sci. U S A 1998, 95, 15665–15670. [PubMed: 9861027] Erratum in: Proc. Natl. Acad. Sci. U S A 1999, 96, 2569.

[31]. Mechetner EB, Roninson IB, Proc. Natl. Acad. Sci. U S A 1992, 89, 5824–5828. [PubMed: 1352877]

[32]. Wieczorek A, Błauż A, Zakrzewski J, Rychlik B, Plażuk D, ACS Med. Chem. Lett 2016, 7, 612–617. [PubMed: 27326336]

[33]. Hollo Z, Homolya L, Davis CW, Sarkadi B, Biochim. Biophys. Acta 1994, 1191, 384–388. [PubMed: 7909692]

[34]. Draper MP, Martell RL, Levy SB, Eur. J. Biochem 1997, 243, 219–224. [PubMed: 9030742]

[35]. Jonker JW, Buitelaar M, Wagenaar E, Van Der Valk MA, Scheffer GL, Scheper RJ, Plosch T, Kuipers F, Elferink RP, Rosing H, Beijnen JH, Schinkel AH, Proc. Natl. Acad. Sci. U S A 2002, 99, 15649–15654. [PubMed: 12429862]

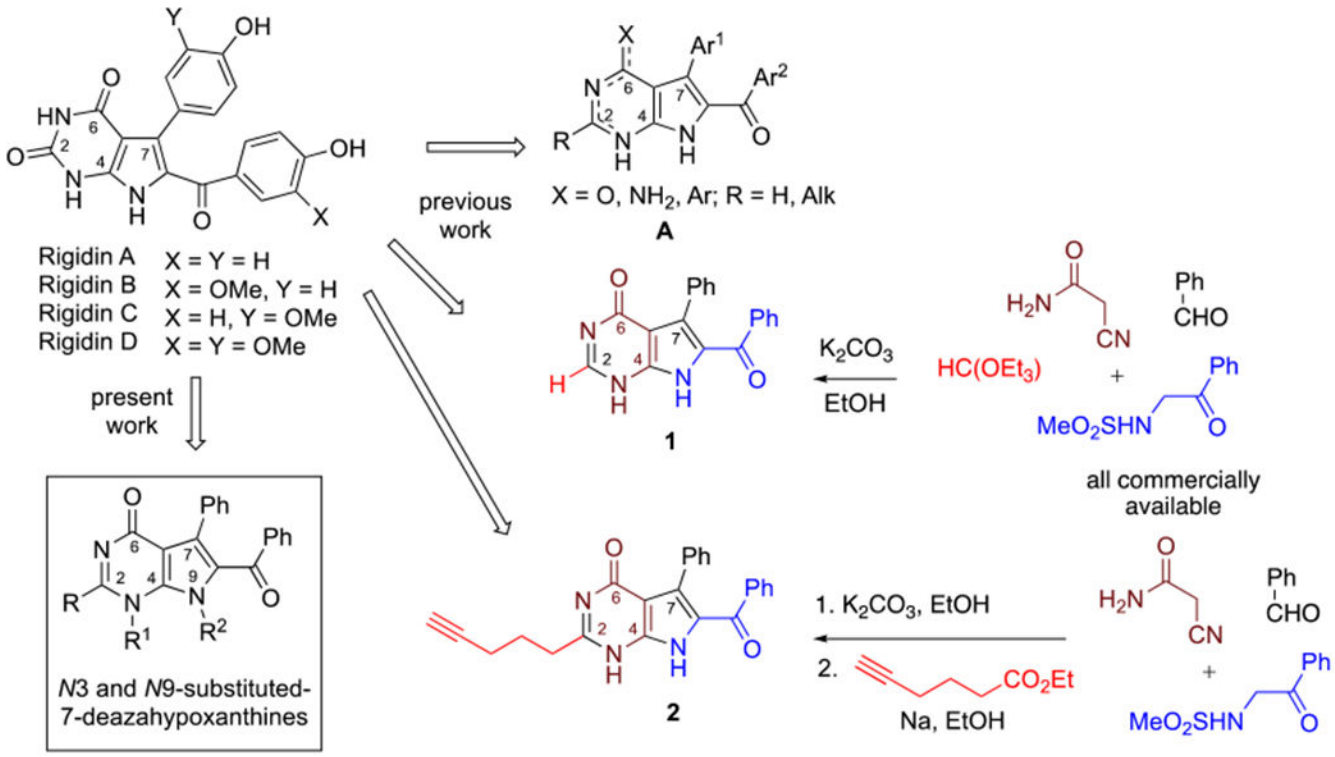

Figure 1.
Systematic SAR investigation of rigidin analogues.

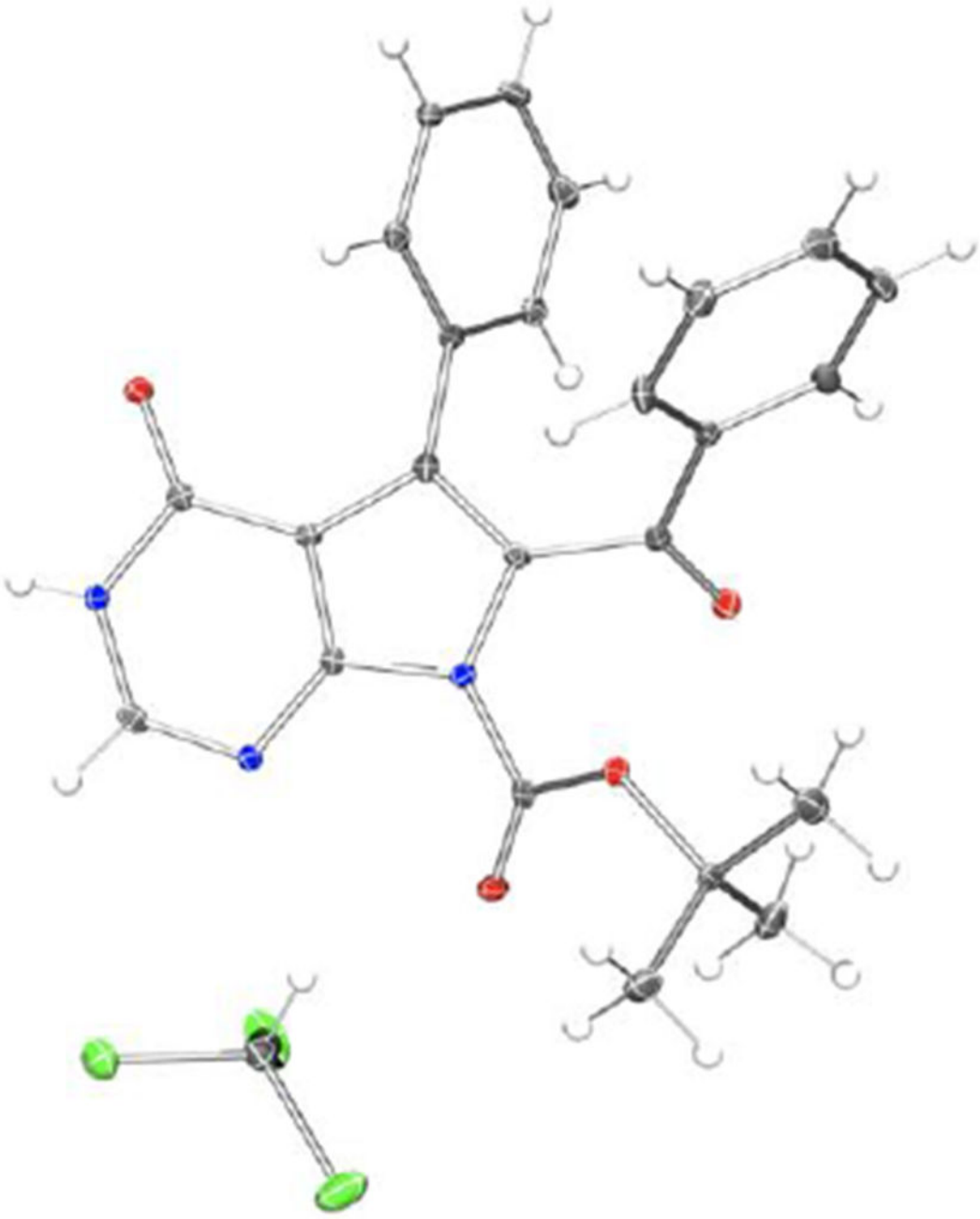

Figure 2.
X-ray structure of **3**·$CHCl_3$. Thermal elipsoids are drawn at the 50% probability level

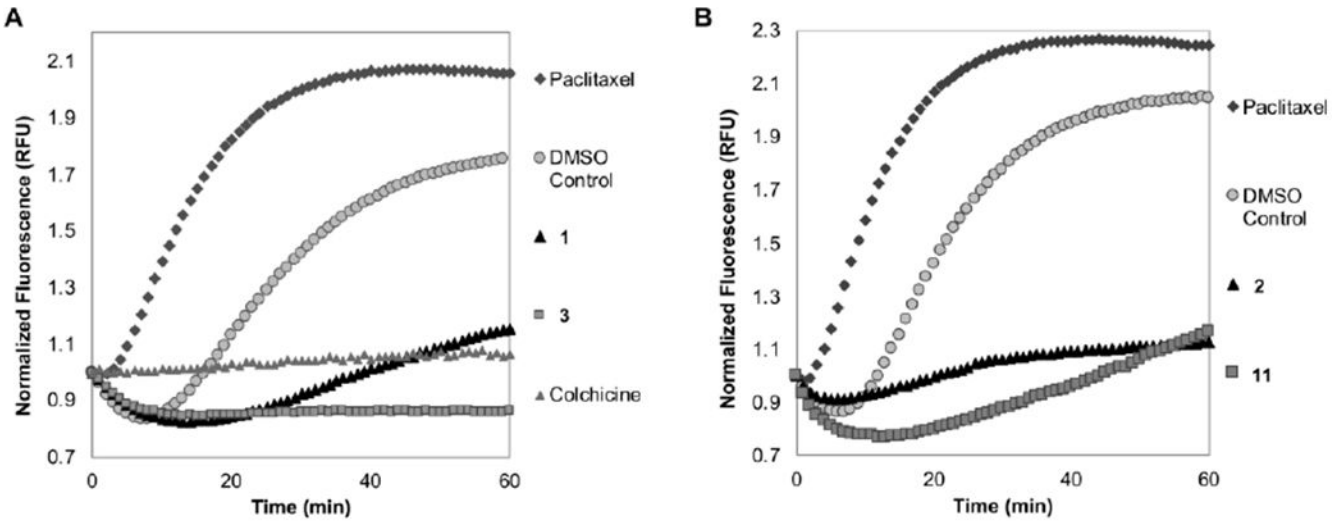

Figure 3.

Effects of compounds **1** and **3** (A), and **2** and **11** (B) on *in vitro* tubulin polymerization. Taxol (3 μM) promotes (A, B), while colchicine (25 μM) suppresses (A) microtubule formation relative to 0.1% DMSO control. **1**, **3**, **2** and **11** (all at 25 μM) suppress tubulin polymerization.

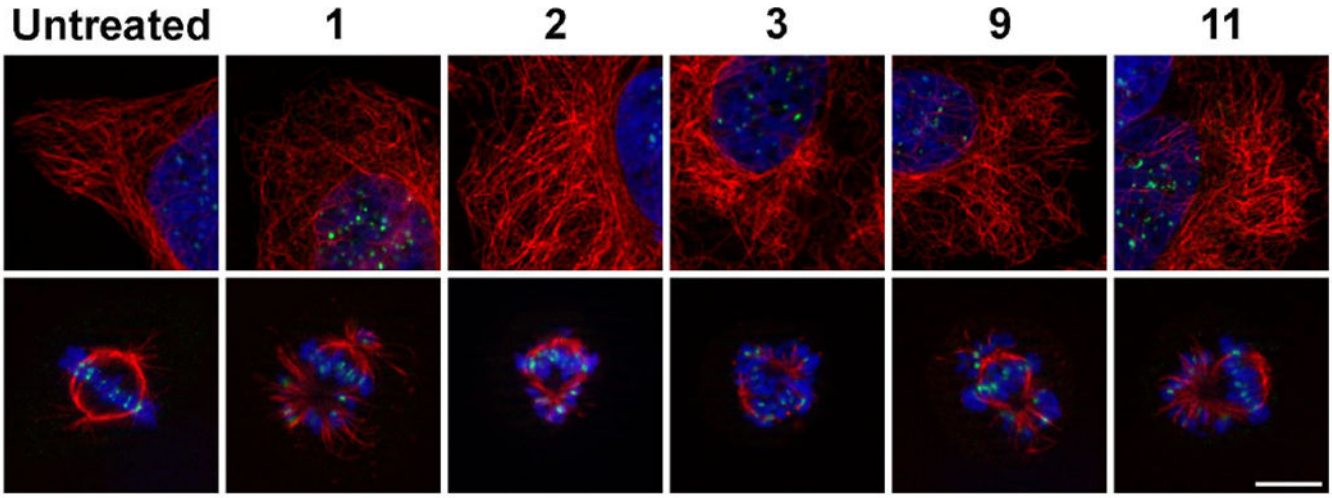

Figure 4.

Microtubule organization in HeLa cells during interphase (top row) and mitosis (bottom row). HeLa cells were treated for 3 h with compounds **1**, **2**, **3**, **9**, **11** at a concentration of 50 nM. Following drug treatment, cells were probed for microtubules (red), centromeres (green) and DNA (blue). Bar, 10 μm.

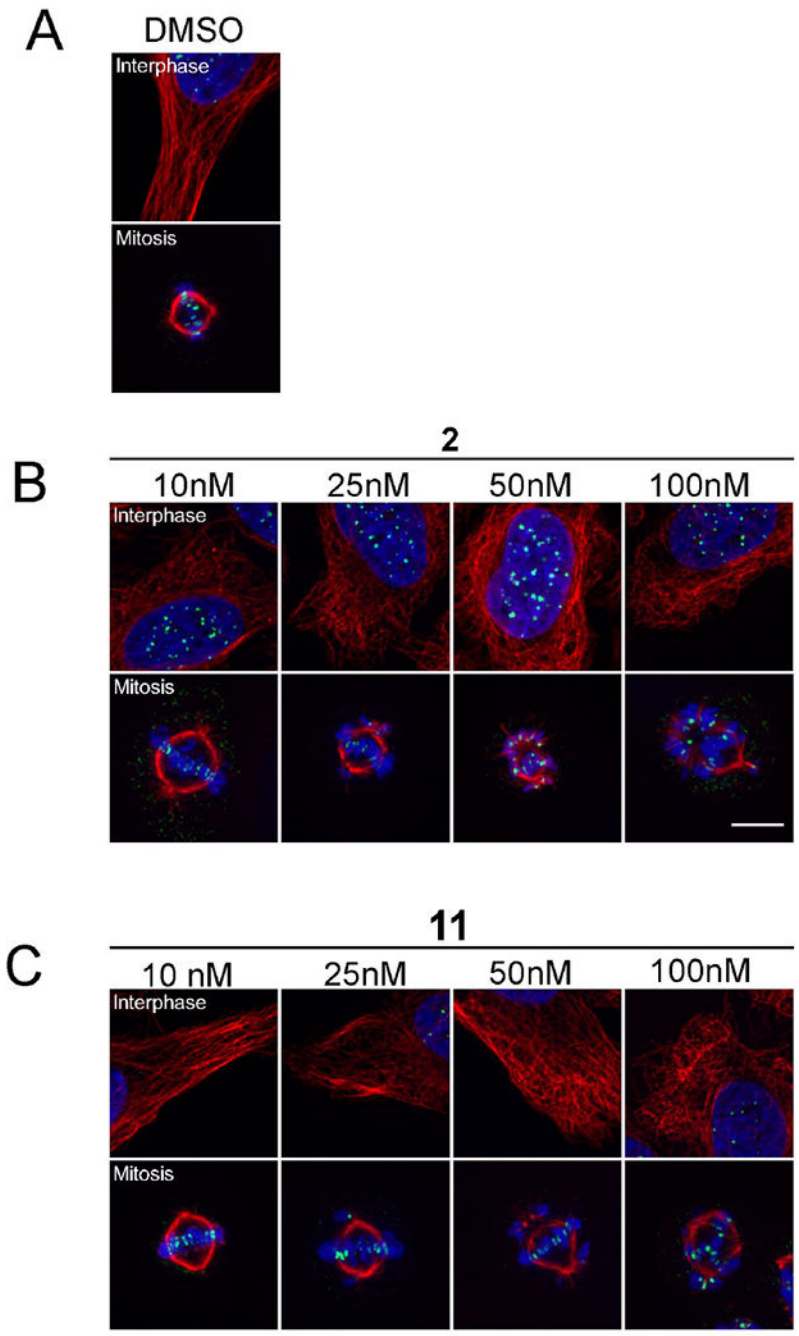

Figure 5.

Microtubule organization in HeLa cells during interphase and mitosis when HeLa cells were treated for 3 h with compounds **2** (B) and its *N*9-*t*-butoxycarbonyl derivative **11** (C) at a range of concentrations. Following drug treatment, cells were probed for microtubules (red), the centromeres (green) and DNA (blue). Bar, 10 μm.

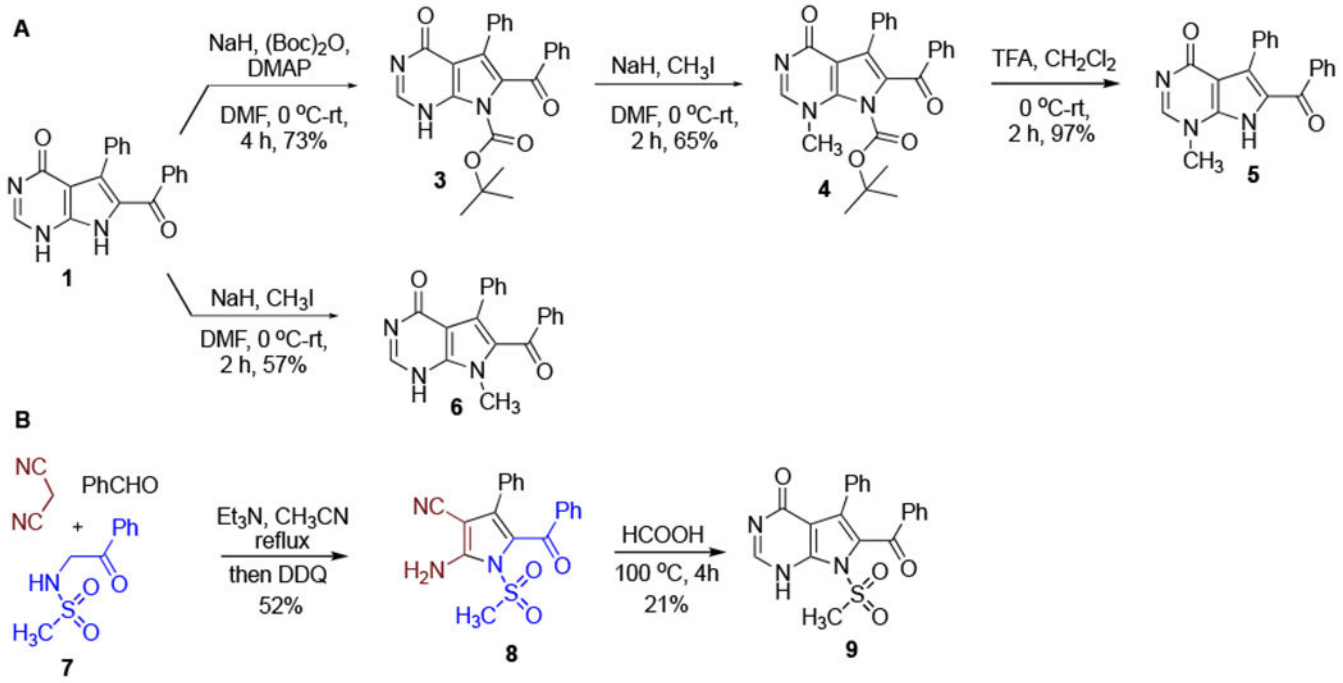

Scheme 1.

Preparation of *N*3- and *N*9-substituted analogues of **1**

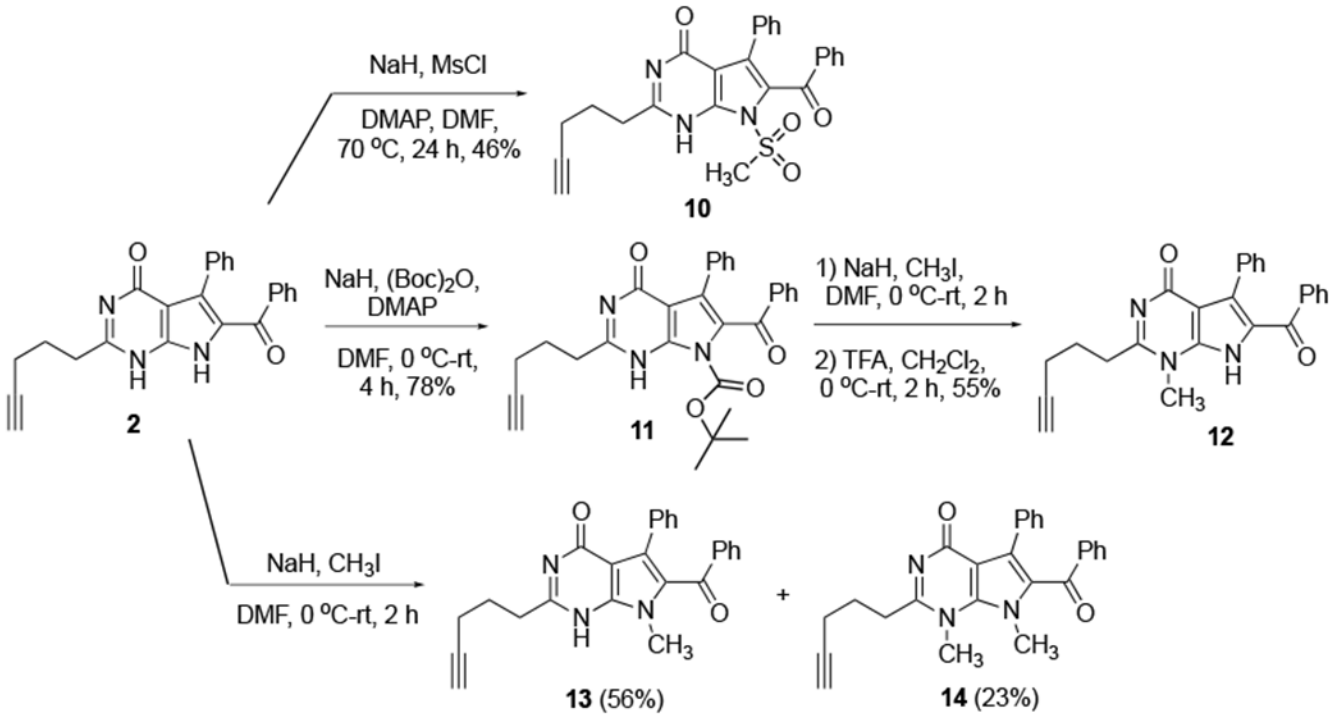

Scheme 2.
Preparation of *N*3- and *N*9-substituted analogues of **2**

Table 1.

Antiproliferative activities of *N*3- and *N*9-substituted analogues of **1** and **2** synthesized in this work

#	structure	cell viability[a] GI_{50}, μM, ± SD		#	structure	cell viability GI_{50}, μM, ± SD	
		HeLa	MCF-7			HeLa	MCF-7
1	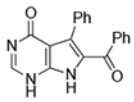	0.035 ± 0.007	0.040 ± 0.024	**2**	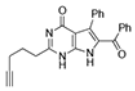	0.022 ± 0.002	0.038 ± 0.018
3	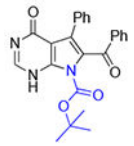	0.029 ± 0.002	0.029 ± 0.001	**10**	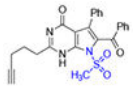	0.11 ± 0.01	0.10 ± 0.01
4	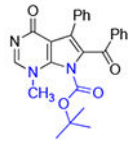	81 ± 3	81 ± 4	**11**	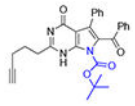	0.021 ± 0.003	0.074 ± 0.005
5	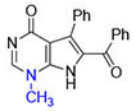	44 ± 2	47 ± 0	**12**	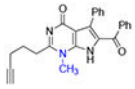	>100	>100
6	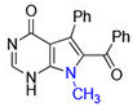	2.8 ± 0.6	5.8 ± 0.1	**13**	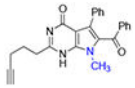	10.3 ± 0.5	20.6 ± 5.5
9	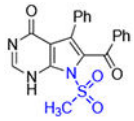	0.028 ± 0.001	0.029 ± 0.001	**14**	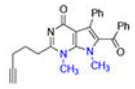	29.2 ± 3.5	45.4 ± 3.4

[a]Concentration required to reduce the viability of cells by 50% after a 48 h treatment with the indicated compounds relative to a DMSO control ± SD from two independent experiments, each performed in 4 replicates, as determined by the MTT assay.

Table 2.

Cytotoxic effects of rigidin analogues in the SW620 cell line panel.

SW620	SW620C	SW620D	SW620E	SW620M	SW620V
			2		
159.9[a]	178.4	207.8	192.7	137.7	186.0
133.6 – 191.4	140.8 – 226.1	176.6 – 244.4	154.6 – 240.2	117.6 – 161.3	157.6 – 219.5
			3		
116.9	160.0	97.4	76.5	92.8	74.5
76.5 – 178.7	97.3 – 263.2	56.8 – 167.1	46.3 – 126.6	53.8 – 159.9	47.1 – 117.6
			11		
30.5	84.8	68.0	118.7	20.3	81.5
17.2 – 54.1	45.8 – 157.1	40.2 – 115.0	65.8 – 214.1	11.7 – 35.4	55.4 – 119.9
			1		
90.5	101.8	128.1	103.4	123.5	134.3
51.5 – 159.0	69.2 – 149.8	87.2 – 188.3	72.2 – 148.1	87.8 – 173.8	98.0 – 184.1

[a]The results (GI_{50} in nM) are presented along with their respective 95% confidence intervals (lower line). Calculations were performed using data obtained in three independent experiments.

Table 3.

Cytotoxic effects of rigidin analogues in MDCKII cell line panel.

MDCKII	MDCKII-BCRP	MDCKII-MDR
	2	
~ 24.1[a]	16.8	21.1
(Very wide)	14.5 – 19.4	19.3 – 23.0
	3	
15.2	14.2	15.0
11.7 – 19.8	13.5 – 15.0	14.1 – 15.9
	11	
18.3	14.2	18.9
14.4 – 23.3	12.8 – 15.8	17.3 – 20.7
	1	
15.8	15.0	17.3
13.5 – 18.5	14.2 – 15.8	15.0 – 20.1

[a]The results (GI_{50} in nM) are presented along with their respective 95% confidence intervals (lower line). Calculations were performed using data obtained in three independent experiments.

Table 4.

Possible modulatory effects of rigidin analogues on mitoxantrone and vincristine resistance in, respectively, MDCKII-BCRP and MDCKII-MDR1 cells.

Mitoxantrone toxicity											
MDCKII	**MDCKII +Ko143**	**MDCKII +2**	**MDCKII +3**	**MDCKII +11**	**MDCKII +1**	**MDCKII-BCRP**	**MDCKII-BCRP +Ko143**	**MDCKII-BCRP +2**	**MDCKII-BCRP +3**	**MDCKII-BCRP +11**	**MDCKII-BCRP +1**
18.7[a]	21.3	14.5	17.4	15.0	16.9	149.3	44.6	145.7	165.0	131.6	126.5
14.7 – 23.8	12.2 – 37.3	11.9 – 17.6	13.6 – 22.2	11.5 – 19.5	13.4 – 21.4	117.4 – 189.8	35.6 – 56.0	120.8 – 175.9	133.3 – 204.2	113.8 – 152.1	109.2 – 146.6
Vincristine toxicity											
MDCKII	**MDCKII +Ver**	**MDCKII +2**	**MDCKII +3**	**MDCKII +11**	**MDCKII +1**	**MDCKII-MDR**	**MDCKII-MDR +Ver**	**MDCKII-MDR +2**	**MDCKII-MDR +3**	**MDCKII-MDR +11**	**MDCKII-MDR +1**
11.5	11.1	10.5	11.8	11.8	11.8	434.0	15.5	409.3	442.6	321.6	397.5
10.9 – 12.1	10.1 – 12.2	9.9 – 11.2	10.0 – 13.8	11.0 – 12.7	10.7 – 13.0	366.2 – 514.4	14.2 – 16.9	334.1 – 501.4	376.7 – 520.1	259.3 – 398.8	327.7 – 482.1

[a]The results (GI_{50} in nM) are presented along with their respective 95% confidence intervals (lower line). Calculations were performed using data obtained in three independent experiments.

Table 5.

Direct effects of rigidin analogues on multidrug resistance protein activity.

Calcein accumulation rate (ABCB1 activity) [AU/min]											
SW620	**SW620 +Ver**	**SW620 +2**	**SW620 +3**	**SW620 +11**	**SW620 +1**	**SW620V**	**SW620V +Ver**	**SW620V +2**	**SW620V +3**	**SW620V +11**	**SW620V +1**
42659 ± 1464[a]	43073 ± 880	36190 ± 408	41254 ± 407	23220 ± 2593	26393 ± 2656	297 ± 31	25416 ± 451	319 ± 33	385 ± 47	299 ± 32	314 ± 50
Pheophorbide *a* accumulation rate (ABCG2 activity) [AU/min]											
SW620	**SW620 +Ko143**	**SW620 +2**	**SW620 +3**	**SW620 +11**	**SW620 +1**	**SW620C**	**SW620C +Ko143**	**SW620C +2**	**SW620C +3**	**SW620C +11**	**SW620C +1**
34224 ± 3361	30113 ± 3023	30922 ± 2994	31938 ± 2971	32380 ± 2769	30778 ± 2946	17493 ± 1621	36522 ± 3314	15277 ± 1409	16572 ± 1769	17871 ± 1309	14248 ± 1292
BCECF half-life in the cell (ABCC1 activity) [min]											
SW620	**SW620 +MK571**	**SW620 +2**	**SW620 +3**	**SW620 +11**	**SW620 +1**	**SW620M**	**SW620M +MK571**	**SW620M +2**	**SW620M +3**	**SW620M +11**	**SW620M +1**
33.36	49.55	38.88	39.69	47.51	38.15	16.09	68.39	20.46	17.21	17.12	17.41
8.89 - ∞	10.76 - ∞	9.72 - ∞	9.43 - ∞	10.31 - ∞	9.82 - ∞	5.48 - ∞	21.06 - ∞	6.64 - ∞	5.75 - ∞	5.93 - ∞	5.75 - ∞

[a]Mean values ± standard deviations are presented except for BCECF assay where 95% confidence interval is presented (lower line). Averaged data for three independent experiments.